Applied Physics Letters

Spatial structure of $In_{0.25}Ga_{0.75}As/GaAs/GaP$ quantum dots on the atomic scale

Cite as: Appl. Phys. Lett. **102**, 123102 (2013); https://doi.org/10.1063/1.4798520
Submitted: 22 January 2013 • Accepted: 14 March 2013 • Published Online: 25 March 2013

Christopher Prohl, Andrea Lenz, Dominik Roy, et al.

Spatial structure of $In_{0.25}Ga_{0.75}As$/GaAs/GaP quantum dots on the atomic scale

Christopher Prohl,[a] Andrea Lenz, Dominik Roy, Josephine Schuppang, Gernot Stracke, André Strittmatter, Udo W. Pohl, Dieter Bimberg, Holger Eisele, and Mario Dähne
Technische Universität Berlin, Institut für Festkörperphysik, Hardenbergstr. 36, 10623 Berlin, Germany

(Received 22 January 2013; accepted 14 March 2013; published online 25 March 2013)

$In_{0.25}Ga_{0.75}As$/GaAs quantum dots grown by metalorganic vapor-phase epitaxy in a GaP matrix have been investigated on the atomic scale using cross-sectional scanning tunneling microscopy. The quantum dots have a truncated pyramidal shape with a reversed cone stoichiometry profile. All deposited indium is found within the quantum dots and the occasionally observed quantum rings, while the wetting layer has a GaAsP composition without any indium inside. This indicates an intense lateral material transfer during growth. © *2013 American Institute of Physics*.
[http://dx.doi.org/10.1063/1.4798520]

The growth and properties of In(Ga)As quantum dots in a GaAs matrix have been extensively studied, leading to a variety of applications in semiconductor opto-electronics.[1] GaP as a matrix material has recently come into focus due to a small lattice mismatch of less than 0.4% to silicon, enabling pseudomorphic growth of GaP on silicon substrates.[2] Developing semiconductor nanostructures such as InGaAs quantum dots in a GaP matrix will offer the possibility of direct integration of III-V opto-electronic devices into silicon-based technology. Furthermore, InGaAs/GaP quantum dots are interesting for new nano-memory cells due to their expected high hole-localization energies,[3] promising long storage times for DRAM with high structural density.[4]

The exploration of suitable growth conditions in this highly strained In(Ga)As/GaP system proved to be very challenging.[4–8] For a detailed understanding of the growth processes and for improving the opto-electronic properties, the knowledge about the resulting atomic structure is essential. Here, we applied cross-sectional scanning tunneling microscopy (XSTM) as a powerful tool to obtain atomically resolved structural data of InGaAs/GaAs/GaP(001) nanostructures.

The sample was grown by metalorganic vapor-phase epitaxy on a GaP(001) substrate. It contains a stack of three InGaAs/GaAs layers grown at 500 °C, each consisting of nominally 3.0 monolayers (ML) GaAs followed by 2.0 ML of $In_{0.25}Ga_{0.75}As$ and a growth interruption of 10 s [see Fig. 1(a)]. The GaAs layer deposited prior to the InGaAs layer was used to induce the Stranski-Krastanov growth mode, leading to quantum-dot formation.[4] The three $In_{0.25}Ga_{0.75}As$/GaAs layers are separated from each other by 50 nm undoped GaP to prevent strain-induced alignment. Finally, a 10-fold superlattice of 2.0 ML GaAs and 10 nm GaP was grown on top at 600 °C, in order to study the growth of the GaAs interlayers separately without the influence of the InGaAs deposition.

The XSTM experiment was performed using a customized instrument with an RHK Technology SPM 1000 control unit. Clean (110) surfaces were obtained by cleavage under ultrahigh vacuum conditions at a base pressure below 1×10^{-8} Pa. Electrochemically etched tungsten wires were used as tips, which were further cleaned *in situ* by electron bombardment.

A filled-state XSTM overview image across the (110) cleavage surface is shown in Fig. 1(b). The three $In_{0.25}Ga_{0.75}As$/GaAs layers can be easily identified as stripes of bright contrast, being separated by about 50 nm of GaP. The bright contrast originates from the higher lattice parameter of InGaAs and GaAs as compared with GaP, leading to an outward relaxation (structural contrast) of the compressively strained layers after sample cleavage. In addition, the low-dimensional states of InGaAs and GaAs in GaP contribute to an increased tunneling probability as compared with the GaP matrix (electronic contrast) and thus a related bright image contrast.[9]

The contrast in each of the $In_{0.25}Ga_{0.75}As$/GaAs layers is not homogeneous along the $[\bar{1}10]$ direction. Instead localized regions of brighter contrast are visible, indicating the formation of quantum dots. In between these quantum dots, an intermediate contrast is found, which is related to the wetting layer. The structural findings indicate a Stranski-Krastanov growth mode for the investigated InGaAs/GaAs/GaP system. From a statistical analysis of the nanostructure occurrence across several XSTM overview images the areal density was determined to about 2.4×10^{11} cm^{-2} for the nanostructures in each layer.

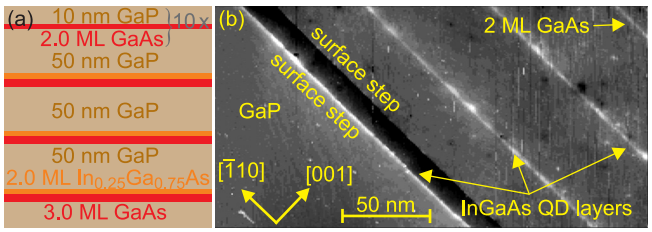

FIG. 1. (a) Schematic of the investigated sample showing the nominally grown layers. (b) Filled-state XSTM overview image showing the three $In_{0.25}Ga_{0.75}As$/GaAs layers as well as one GaAs layer in the GaP matrix. In addition two monoatomic surface steps are visible, one very close to the first InGaAs quantum-dot layer. The image was taken at a sample voltage $V_T = -2.5$ V and a tunneling current $I_T = 50$ pA.

[a]Author to whom correspondence should be addressed. Electronic mail: Christopher.Prohl@physik.tu-berlin.de

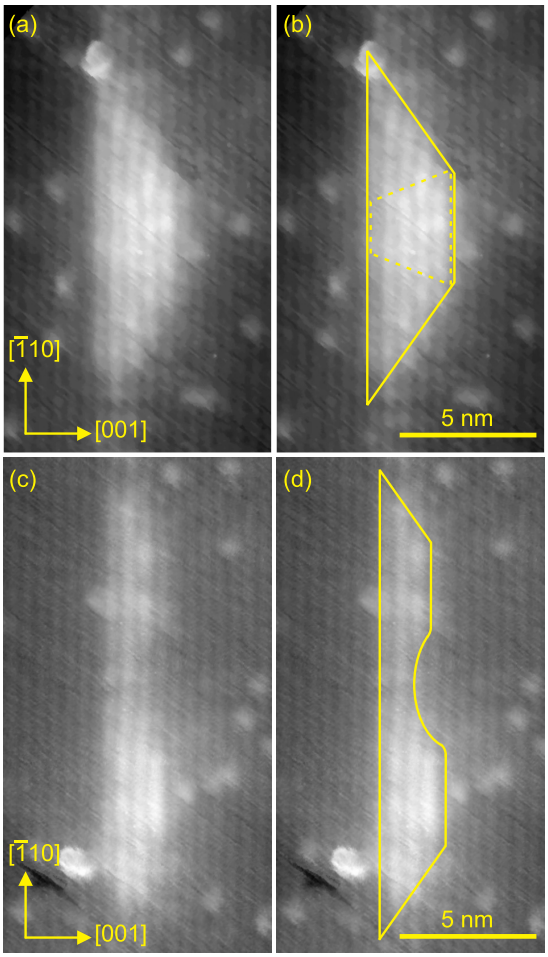

FIG. 2. Filled-state XSTM images of (a),(b) a quantum dot and (c),(d) a quantum ring. The images were taken at $V_T = -3.0$ V and $I_T = 30$ pA. The contours of the nanostructures are marked by the solid lines. The dashed line in (b) marks the indium-rich area. The bright spots on top of the GaP surface are supposed to be phosphorous adatoms pulled out of the cleavage surface during the scanning process (see Ref. 15).

Figure 2 shows high-resolution filled-state XSTM images of different single nanostructures. A typical quantum dot is shown in Figs. 2(a) and 2(b). It has a trapezoidal cross section, as highlighted by the solid lines in Fig. 2(b), indicating a truncated pyramidal shape. Such a truncated pyramidal shape is typical for capped quantum dots and was already found for other material systems like InAs/GaAs.[10–14] The average quantum-dot base length is found to be 12 nm, and quantum-dot heights up to 10 ML are observed.

In some cases, two smaller trapezoidal cross sections appear very close to each other or even overlap as, e.g., shown in Figs. 2(c) and 2(d). This kind of appearance was already occasionally observed in experiments growing In(Ga)As on GaAs,[11] but more frequently for GaSb on GaAs.[16] Such a cross-sectional shape is obtained by cleaving through so-called quantum rings.[16] Since the cleavage through the quantum rings occurs at an arbitrary position, their appearance in XSTM experiments may vary between a double structure for more central cleavages and a single structure—being equivalent to the cross section of a quantum dot—for a cleavage near the side of the quantum ring. Here, the quantum rings show average total base lengths of 21 nm with heights up to 9 ML. Hence, the larger quantum dots transform into quantum rings during growth[16] or capping.[11,17] The similar contrast of quantum dots and rings indicates a comparable chemical composition.

A closer look at Figs. 2(a) and 2(b) also yields a non-uniform contrast within the quantum dots. The dot center is characterized by a significantly brighter contrast than the dot sides. Furthermore, the width of the region with bright contrast is most narrow at the quantum-dot base and broader towards its top. Thus, the area of brighter contrast has the shape of a reversed truncated cone as highlighted by the dashed lines in Fig. 2(b). This contrast is caused by a higher indium concentration at the center as compared with the outer parts of the quantum dot. Such a stoichiometry profile has already been observed for InGaAs quantum dots in a GaAs matrix.[11,18]

Figure 3(a) shows an XSTM filled-state image of a wetting-layer region of one of the $In_{0.25}Ga_{0.75}As$/GaAs layers. The wetting layer appears with heights between 2 and 5 ML and shows an inhomogeneous contrast, being characterized by regions with two different brightnesses. Since the image is measured in filled-state mode—corresponding to negative sample bias—its contrast is mostly sensitive to the group-V sublattice with darker phosphorous and brighter arsenic atoms. The brighter arsenic-rich regions [marked by ovals in Figure 3(a)] are surrounded by darker phosphorous-rich ones. Each of these regions for itself shows a homogeneous brightness which already indicates that no indium is present within the wetting layer.

For a quantitative evaluation of the stoichiometry within the quantum dots and the wetting layer the local lattice parameter along growth direction as derived from the XSTM data can be analyzed.[10,11] For this purpose, the distance of neighboring atomic chains is determined within a selected area and plotted versus the position along growth direction.

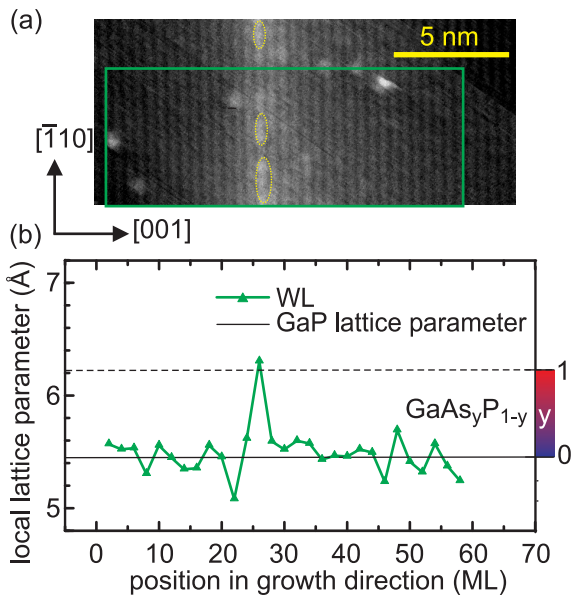

FIG. 3. (a) Filled-state XSTM image of the wetting layer region, taken at $V_T = -3.0$ V and $I_T = 30$ pA. Arsenic-rich regions with brighter contrast are marked by (yellow) ovals. (b) Evaluation of the local lattice parameter along growth direction within the (green) box in (a). The local lattice parameter is related to the local arsenic concentration. The right scale bar and the dashed line in (b) indicate the calculated values for the local lattice parameter for strained GaAsP layers in a GaP matrix.

The resulting graph in Fig. 3(b) shows the local lattice parameter for the selected wetting-layer region of the $In_{0.25}Ga_{0.75}As$/GaAs layer, averaged perpendicular to the growth direction over about 5 nm, as highlighted by the (green) box in Fig. 3(a). The local lattice parameter underneath and above the wetting layer is normalized to the value of the GaP bulk lattice constant of 5.45 Å. The slight variation is of statistical origin, based on, e.g., scanning artefacts or adatoms at the surface. In the area of the wetting layer the local lattice parameter increases considerably due to the change in material composition. The compressive strain originating from the lattice mismatch leads to a relaxation along growth direction (biaxial strain), further increasing the local lattice parameter. The small undershoot before the InGaAs/GaAs deposition in the graph of Fig. 3(b) is characteristic for an inhomogeneity of the wetting-layer composition, as already observed above. The local lattice parameter is found to be increased in a 2–3 ML wide region, in good agreement with the visual appearance of the wetting layer in the XSTM image showing local heights of 2–5 ML in growth direction.

For a quantitative analysis of the local stoichiometry, the local lattice parameter for GaAsP layers of different composition within a GaP matrix was calculated using continuum-mechanical strain-relaxation on a biaxially strained system. The resulting relation between the local lattice parameter and the arsenic concentration y is shown by the scale bar on the right side in Fig. 3(b). The measured local lattice parameter increases roughly to the calculated value for pure GaAs embedded in GaP, again supporting the above assumption that no indium is present within the wetting layer.

In the quantum dots, in contrast, the local lattice parameter clearly shows the incorporation of indium: Figure 4 shows the analysis of the local lattice parameter for the quantum dot shown in Figs. 2(a) and 2(b). In Fig. 4(a) the two graphs correspond to the data derived at the quantum-dot center and at the quantum-dot sides as highlighted by the (blue and red) boxes in the XSTM image in the inset. The local lattice parameter at the quantum-dot center is found to be much higher at the top of the quantum dot than at its base, in good agreement with the stoichiometry profile of the quantum dot already obtained above by visual inspection of the XSTM image contrast.

In Fig. 4(b) the profile of the local lattice parameter averaged over the entire quantum-dot area is shown as highlighted by the (green) box in the inset. The local lattice parameter is compressed underneath the quantum dot and rises to comparably high values within the quantum dot, exceeding the value of GaAs in GaP. This proves the incorporation of indium within the quantum dots during growth. Also, the undershoot below the GaP lattice parameter is much larger as compared with the case of the wetting layer, indicating a stronger compression of the material directly underneath the quantum dot as well as at the quantum-dot base, as compared with the weak compression due to the stoichiometry fluctuations within the wetting layer. Taking this compression into account, the curve is locally corrected as shown in (green) open squares, in order to reflect the actual material concentration within the quantum dot.

In contrast to the wetting layer [see Fig. 3(a)] the filled-state XSTM image contrast for the quantum dots is

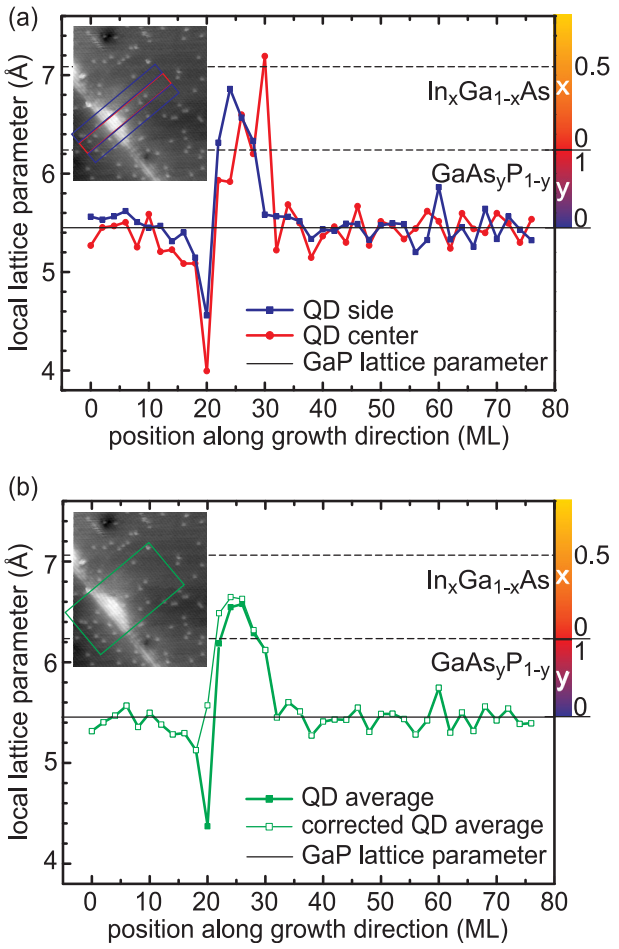

FIG. 4. Evaluation of the local lattice parameter and the related stoichiometric composition along growth direction for a representative quantum dot. The graphs show the evaluated data (a) for the quantum-dot center in (red) dots and for the quantum-dot sides in (blue) squares and (b) averaged over the entire quantum-dot region in (green) squares and the corrected data in (green) open squares. For the latter the compression around the quantum-dot base is taken into account. The evaluated data in each case refer to the highlighted boxes in the XSTM images. The right scale bars and the dashed lines in the graphs indicate the calculated values for the local lattice parameter for strained GaAsP and InGaAs layers in a GaP matrix.

characterized by a much softer variation (see Fig. 2). Therefore, we may assume that no phosphorous is present within the quantum dots, which accordingly consist of InGaAs. From the local lattice parameter now the indium concentration x within the InGaAs quantum dots can be derived, as illustrated by the upper scale bar on the right side in Figs. 4(a) and 4(b). It is found that the average indium concentration inside the entire quantum dot amounts to around 20–25% and reaches up to almost 50% at its top.

Finally, the total material content in the wetting layer and in the quantum dots (including the quantum rings) is derived from the stoichiometry profiles shown in Figs. 3 and 4(b).[19] From an integration of the curves a local amount of 3.1 ML GaAs is found for the wetting layer. On the other hand the total indium content inside the quantum dots is calculated to be around 2 ML. Since about 24% of the growth surface is covered with quantum dots or rings, as derived from their lateral extension and their density, it results that about 2.4 ML of the deposited arsenic is located inside the wetting layer, and a total amount of about 0.5 ML indium is

located in the quantum dots. The latter value nicely agrees with the nominally deposited amount of 0.5 ML indium. As there is no amount of indium left for the wetting layer, this confirms the above assumption that the deposited amount of indium is only located inside the nanostructures.

These material compositions of the wetting layer and the quantum dots are further supported by the graph in Fig. 4(b). If phosphorous was inside the quantum dots, the scale bar for the indium concentration x would shift to lower lattice parameters, resulting in an indium content within the quantum dots even higher than the nominal amount of deposited indium material of 0.5 ML. This consideration additionally confirms that no phosphorous can be present within the quantum dots. The lack of indium material inside the wetting layer for this material system again shows the occurrence of an intense lateral material transport from the wetting layer into the quantum dots during Stranski-Krastanov growth, which is already well-known for In(Ga)As/GaAs (Refs. 11, 14, and 20) and also for GaSb/GaAs.[21]

Since the remaining group-III material in the quantum dots can only be gallium, the total GaAs material within the quantum dots is derived using average quantum-dot heights of 9–10 ML, resulting in 7–8 ML GaAs inside the quantum dots and therewith a GaAs content corresponding to an amount of about 1.8 ML. Together with the GaAs amount within the wetting layer, a total GaAs incorporation of about 4.1 ML can be derived, which is in good agreement with the nominally deposited amount of 4.5 ML.

In conclusion, the atomically resolved XSTM data on the InGaAs/GaAs/GaP material system demonstrate that intense material-redistribution effects occur during growth: The subsequently deposited GaAs and InGaAs layers are not found to be incorporated separately, but they intermix. An evaluation of both the XSTM image contrast and the local stoichiometry showed that the nanostructures consist of InGaAs and contain the whole amount of deposited indium material, while the surrounding wetting layer consists of inhomogeneously distributed GaAsP without any indium. The quantum dots exhibit a so-called reversed-cone stoichiometric profile of InGaAs, while the wetting layer laterally decomposes into areas which are more GaAs-rich and more GaP-rich. The resulting larger quantums dots transform into quantum rings, and both together have a relatively high density of 2.4×10^{11} cm^{-2}.

The authors thank Ernst Lenz for providing software for data evaluation. Financial support was provided by the Deutsche Forschungsgemeinschaft under projects Bi284/29-1 and SFB 787 TP A2 and A4, the Federal Ministry of Economics and Technology (BMWi) under Grant No. 03VWP0059v, and the Federal Ministry of Education and Research (BMBF) under Grant No. 16V0196 (HOFUS).

[1]D. Bimberg and U. W. Pohl, Mater. Today **14**, 388 (2011).
[2]K. Volz, A. Beyer, W. Witte, J. Ohlmann, I. Németh, B. Kunert, and W. Stolz, J. Cryst. Growth **315**, 37 (2011).
[3]L. Pedesseau, J. Even, A. Bondi, W. Guo, S. Richard, H. Folliot, C. Labbe, C. Cornet, O. Dehaese, A. Le Corre, O. Durand, and S. Loualiche, J. Phys. D: Appl. Phys. **41**, 165505 (2008).
[4]G. Stracke, A. Glacki, T. Nowozin, L. Bonato, S. Rodt, C. Prohl, A. Lenz, H. Eisele, A. Schliwa, A. Strittmatter, U. W. Pohl, and D. Bimberg, Appl. Phys. Lett. **101**, 223110 (2012).
[5]R. Leon, C. Lobo, T. P. Chin, J. M. Woodall, S. Fafard, S. Ruvimov, Z. Liliental-Weber, and M. A. S. Kalceff, Appl. Phys. Lett. **72**, 1356 (1998).
[6]S. Fuchi, Y. Nonogaki, H. Moriya, Y. Fujiwara, and Y. Takeda, Jpn. J. Appl. Phys. **39**, 3290 (2000).
[7]Y. Song, P. J. Simmonds, and M. L. Lee, Appl. Phys. Lett. **97**, 223110 (2010).
[8]T. N. Thanh, C. Robert, C. Cornet, M. Perrin, J. M. Jancu, N. Bertru, J. Even, N. Chevalier, H. Folliot, O. Durand, and A. Le Corre, Appl. Phys. Lett. **99**, 143123 (2011).
[9]R. M. Feenstra, Phys. B: Condens. Matter **273**, 796 (1999).
[10]O. Flebbe, H. Eisele, T. Kalka, F. Heinrichsdorff, A. Krost, D. Bimberg, and M. Dähne-Prietsch, J. Vac. Sci. Technol. B **17**, 1639 (1999).
[11]A. Lenz, R. Timm, H. Eisele, C. Hennig, S. K. Becker, R. L. Sellin, U. W. Pohl, D. Bimberg, and M. Dähne, Appl. Phys. Lett. **81**, 5150 (2002).
[12]H. Eisele, A. Lenz, R. Heitz, R. Timm, M. Dähne, Y. Temko, T. Suzuki, and K. Jacobi, J. Appl. Phys. **104**, 124301 (2008).
[13]L. Ivanova, H. Eisele, A. Lenz, R. Timm, M. Dähne, O. Schumann, L. Geelhaar, and H. Riechert, Appl. Phys. Lett. **92**, 203101 (2008).
[14]H. Eisele, Ph. Ebert, N. Liu, A. L. Holmes, Jr., and C.-K. Shih, Appl. Phys. Lett. **101**, 233107 (2012).
[15]Ph. Ebert and K. Urban, Ultramicroscopy **49**, 344 (1993).
[16]R. Timm, H. Eisele, A. Lenz, L. Ivanova, G. Balakrishnan, D. L. Huffaker, and M. Dähne, Phys. Rev. Lett. **101**, 256101 (2008).
[17]J. M. García, G. Medeiros-Ribeiro, K. Schmidt, T. Ngo, J. L. Feng, A. Lorke, J. Kotthaus, and P. M. Petroff, Appl. Phys. Lett. **71**, 2014 (1997).
[18]N. Liu, J. Tersoff, O. Baklenov, A. L. Holmes, Jr., and C. K. Shih, Phys. Rev. Lett. **84**, 334 (2000).
[19]A. Lenz, H. Eisele, J. Becker, L. Ivanova, E. Lenz, F. Luckert, K. Pötschke, A. Strittmatter, U. W. Pohl, D. Bimberg, and M. Dähne, Appl. Phys. Express **3**, 105602 (2010).
[20]C. Prohl, B. Höpfner, J. Grabowski, M. Dähne, and H. Eisele, J. Vac. Sci. Technol. B **28**, C5E13 (2010).
[21]L. Müller-Kirsch, R. Heitz, U. W. Pohl, D. Bimberg, I. Häusler, H. Kirmse, and W. Neumann, Appl. Phys. Lett. **79**, 1027 (2001).